Available online at www.eccomasproceedia.org
Eccomas Proceedia COMPDYN (2021) 2488-2497

ECCOMAS
Proceedia

COMPDYN 2021
8th ECCOMAS Thematic Conference on
Computational Methods in Structural Dynamics and Earthquake Engineering
M. Papadrakakis, M. Fragiadakis (eds.)
Streamed from Athens, Greece, 28 - 30 June 2021

SEISMIC ISOLATION OF LIGHTWEIGHT STRUCTURES THROUGH WIRE ROPE DEVICES: PRELIMINARY EXPERIMENTAL RESULTS AND SIMULATION

Mariacristina Spizzuoco[1], **and Giorgio Serino**[1]

[1] Department of Structures for Engineering & Architecture, University of Napoli Federico II
Via Claudio 21, 80125 Naples, Italy
e-mail: spizzuoc@unina.it

Abstract

The work presents some preliminary results of experimental tests performed on a Helical Wire Rope Isolator (HWRI), to the aim of describing the dynamic behavior of the metal isolation device, without pre-load and under the effect of a vertical pre-load, for different displacement amplitudes. During the dynamic tests, the testing machine allows to apply a vertical displacement or load history to the tested device, subjected to a constant vertical pre-load. The dynamic behavior of the tested device depends on the applied displacement amplitude: the HWRI displays an asymmetric behaviour, i.e. a different response when it is subjected to compression or tension; in the latter case, it shows an hardening effect for larger displacements. Moreover, the experimental tests make clear that the application of a vertical pre-load determines a different behaviour in Compression vs. Tension, with slightly variable damping properties. In order to simulate the dynamic behavior of the HWRIs in Compression-Tension direction, a nonlinear model is proposed, that is validated by comparing the experimental hysteresis loops obtained during cyclic tests with those predicted analytically.

Keywords: Base Isolation, Experimental Dynamic Characterization, Wire-Rope Isolators.

ISSN:2623-3347
Peer-review under responsibility of the organizing committee of COMPDYN 2021.
doi:10.7712/120121.8652.18879

1 INTRODUCTION

Helical Wire Rope Isolators (HWRI) are metal devices which are effective in protecting sensitive equipment from shock and vibration [1], so that they are frequently used as devices for the earthquake protection of that equipment installed in buildings [2] and for the reduction of seismic vibration induced on high voltage ceramic circuit breakers [3-6]. But, they have been also adopted as vertical isolators under the basement of the two statues known as "Bronzes of Riace" [7].

HWRIs are made of a stainless steel cable embedded into two aluminum alloy or steel retainer bars. They can deform in both vertical and horizontal directions and they have a significant dissipation capacity caused by the inner sliding friction and rubbing among the various strand's wires and among the intertwined strands [1]. The mechanical behavior of HWRIs depend on their geometrical characteristics: the height to width ratio, the device's diameter, the number of strands, the cable length and twist, the number of cables per section and the number of loops [2].

A HWR Isolator, manufactured by Powerflex s.r.l (Limatola, Italy), has been experimentally investigated in its vertical direction, named Compression/Tension. The aim of the experimental tests was to study the dynamic behaviour of the considered device in a quite large displacements range, by assigning four different values to the vertical pre-load. Literature shows the results of experimental tests performed within a relatively small displacements range [2, 6, 8].

The experimental investigation of the tested HWRI has been carried out by operating a testing machine available at the Laboratory of Department of Structures for Engineering and Architecture of the University of Naples Federico II. Its dynamic behavior has been studied by analyzing the values assumed by two parameters computed from the experimental hysteresis loops: the average effective (or secant) stiffness in both Compression and Tension, and the average equivalent viscous damping ratio.

2 HELICAL WIRE ROPE ISOLATOR UNDER TESTING

HWRIs are metal devices that are obtained by wounding a wire rope in the form of a helix and embedding into two drilled metal retainer bars. The rope is given by the layering of several strands around a central one. The HWRIs manufactured by Powerflex S.r.l (Limatola, Italy), have a rope that is composed by six strands, each consisting in 25 wires, and a central strand with 49 wires. The cable is made of stainless steel type 316, whereas the material of the retainer bars is an aluminum alloy.

Figure 1 shows the geometrical characteristics of the tested HWRI and the indication of the tested vertical direction: Compression/Tension.

Table 1 lists the geometrical characteristics (cable's diameter, length, width and height of the device) of the tested devices: HWRI PWHS16010 and HWRI PWHS16040.

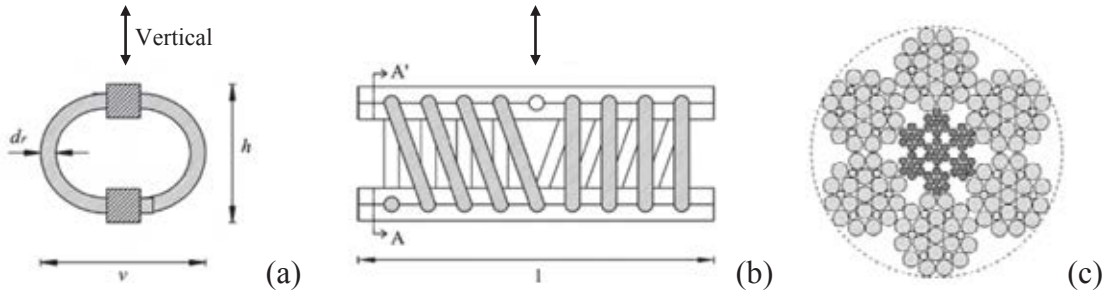

Figure 1: Mount of a wire rope (a); helical configuration of the cable (b); stranded cable's cross section (c).

HWRI	l [mm]	h [mm]	v [mm]	h/v	d_r [mm]
PWHS 16010	267	100	110	0.90	16
PWHS 16040	267	125	150	0.83	16

Table 1: Geometrical characteristics of the HWRIs selected for experimental tests.

3 TESTING MACHINE FOR COMPRESSION/TENSION TESTS

The dynamic experimental tests on the selected HWRIs in Compression/Tension direction have been carried out through a testing machine (Figure 2) available at the Department of Structures for Engineering and Architecture of the University of Naples Federico II (Italy): an MTS Series 370 Servohydraulic Load Frame. The load frame is suitable to perform tests in compression and tension. It includes an axial hydraulic actuator with a maximum capacity of 250 kN and a stroke of 150 mm. Both displacement and force controlled procedures can be followed. In the configuration shown in Figure 2, the dynamic actuator is mounted on the upper crosshead, while a load cell is mounted below the lower hydraulic wedge. The data acquisition system along with the control of the hydraulic actuator are performed with a software running on a personal computer. For Compression/Tension tests, the steel retainer bars of the isolator are gripped by the upper and lower rigid steel parts of the machine. All tests were conducted by imposing vertical displacements at room temperature and the data were sampled at 102.4 Hz. The relative vertical displacement and vertical load time histories have been measured.

Figure 2: Testing machine and the HWRI mounted in vertical direction.

4 EXPERIMENTAL CHARACTERIZATION TESTS

Cyclic tests have been carried out in order to understand the influence of displacement amplitude and vertical pre-load on the dynamic behavior of the selected HWRIs in vertical (Compression/Tension) direction. Nine different displacement amplitudes, four vertical pre-

load values and a testing frequency of 0.1 Hz have been assumed, where the maximum amplitude has been chosen to prevent damage to the aluminum alloy retainer bars. The testing protocol consisted in applying ten fully reversed sinusoidal cycles of vertical displacement, having specified amplitude *A* and frequency *f*, while a constant vertical pre-load was applied to the device. The dynamic displacement-controlled tests are listed in Table 2.

No. of Tests	Frequency [Hz]	Amplitude [mm]	Vertical Load [kN]
HWRI PWHS 16010			
6	0.1	2.5, 5, 7.5, 10, 12.5, 15	0
6	0.1	2.5, 5, 7.5, 10, 12.5, 15	2
HWRI PWHS 16040			
6	0.1	5, 10, 15, 20, 25, 30	0
6	0.1	5, 10, 15, 20, 25, 30	1.2
6	0.1	5, 10, 15, 20, 25, 30	2
6	0.1	5, 10, 15, 20, 25, 30	3

Table 2: Dynamic tests in vertical direction.

5 EXPERIMENTAL TESTS OUTCOMES

The results of the dynamic experimental tests performed on the investigated HWRI PWHS 16040 are presented in this paragraph. The dynamic parameters evaluated from the asymmetric experimental force-displacement hysteresis loops are the average effective (or secant) stiffness values in Compression and Tension, and the average equivalent viscous damping ratio. The effective stiffnesses in Compression and in Tension, corresponding to each load cycle of a dynamic test, have been evaluated based on the peak vertical load and displacement [10], both on Compression side and on Tension side:

$$k_{eff,\mathrm{T}} = \frac{f_{\max}}{u_{\max}} \qquad k_{eff,\mathrm{C}} = \frac{f_{\min}}{u_{\min}} \tag{1}$$

where f_{max}, f_{min}, u_{max}, and u_{min} are the peak values of vertical load and displacement, respectively, at the extremes of the cyclic displacement range. The average effective stiffnesses $k_{eff,\mathrm{T\_a}}$ and $k_{eff,\mathrm{C\_a}}$ have been calculated as mean values of those obtained from seven of the ten experimental loading cycles. The equivalent viscous damping ratio of the device at each cycle has been evaluated as [11, 12]:

$$\xi_{eq} = \frac{1}{\pi}\frac{E_d}{\left(A_{sT} + A_{sC} + A_{rect}\right)} \tag{2}$$

where E_d represents the dissipated energy, that is, the area within the asymmetric hysteresis loop, and A_{sT}, A_{sC} and A_{rect} are the following areas:

$$\mathrm{A_{sT}} = \frac{1}{2}\mathrm{k_{eff,T}}\, u_{\max}^2 \;, \quad \mathrm{A_{sC}} = \frac{1}{2}\mathrm{k_{eff,C}}\, u_{\min}^2 \;, \quad \mathrm{A}_{rect} = u_{\max} \cdot f_{\min} \tag{3}$$

with $u_{\max} = u_{\min}$ the positive and negative maximum displacements, and $f_{\min}$ the negative peak value of vertical load. The average equivalent viscous damping ratio $\xi_{eq,a}$ has been calculated as mean value of those obtained from seven of the ten loading cycles applied to the device.

Regarding the influence of the displacement amplitude on the dynamic behavior of the tested HWRI, Table 3 presents the values of the average effective stiffnesses and the equivalent viscous damping ratio obtained for six different amplitudes without the effect of the vertical pre-load. It can be observed that the tested metal device displays higher effective

stiffnesses and equivalent damping ratio at smaller displacements. The effective stiffness in Compression and the equivalent damping ratio decrease with increasing displacement amplitude, whereas the effective stiffness in Tension increases dramatically at the largest amplitudes. Figure 3 shows the asymmetric force-displacement hysteresis loops obtained in Compression/Tension direction (compression and tension are assumed, respectively, negative and positive) for all six different values of amplitude, for $f = 0.1$ Hz and without the effect of the vertical pre-load. It is worth to note that the shape of the hysteresis loops changes according to the displacement amplitude: at the smallest amplitude the hysteresis loops display a softening stiffness in Compression and a slightly hardening stiffness in Tension, whereas at the highest amplitude the experimental cycles exhibit a stronger nonlinear stiffening behavior only on Tension side.

$P_v = 0$ kN, $f = 0.1$ Hz	Amplitude [mm]	k_{eff,C_a} [N/m]	k_{eff,T_a} [N/m]	$\xi_{eq,a}$ [%]
Compression/Tension	5	859659	1238110	22.7
Compression/Tension	10	576639	1038541	17.5
Compression/Tension	15	454733	999633	15.0
Compression/Tension	20	386610	1023578	13.5
Compression/Tension	25	341244	1114642	12.4
Compression/Tension	30	305053	1343628	11.4

Table 3: Influence of displacement amplitude.

As regards to the effect of the vertical pre-load on the dynamic behavior of the tested metal device, Tables 4 and 5 show the results obtained in Compression/Tension direction for four different values of vertical pre-load, by applying a sinusoidal harmonic motion having frequency of 0.1 Hz and amplitude equal to 15 mm and 30 mm, respectively. From the examination of the outcomes, it can be deduced that, in the case of an intermediate displacement amplitude (15 mm), an increase in the pre-load produces a reduction in the average effective stiffnesses and an approximately constant equivalent viscous damping ratio (Table 4).

$A = 15$ mm, $f = 0.1$ Hz	Vertical Load [kN]	k_{eff,C_a} [N/m]	k_{eff,T_a} [N/m]	$\xi_{eq,a}$ [%]
Compression/Tension	0.0	454733	999633	15.0
Compression/Tension	1.2	406447	864757	14.6
Compression/Tension	2.0	410924	878796	15.0
Compression/Tension	3.0	413397	894691	14.7

Table 4: Influence of vertical load for $A = 15$ mm.

On the other hand, in the case of a larger displacement amplitude (30 mm), an increase in the vertical pre-load produces a strong increase of the average effective stiffness in Tension while the variation of the stiffness in Compression is negligible, and determines a slight decrease of the equivalent viscous damping ratio (Table 5).

$A = 30$ mm, $f = 0.1$ Hz	Vertical Load [kN]	k_{eff,C_a} [N/m]	k_{eff,T_a} [N/m]	$\xi_{eq,a}$ [%]
Compression/Tension	0.0	305453	1343628	11.4
Compression/Tension	1.2	304997	1693672	10.6
Compression/Tension	2.0	305366	1736038	10.0
Compression/Tension	3.0	307147	1943828	9.5

Table 5: Influence of vertical load for $A = 30$ mm.

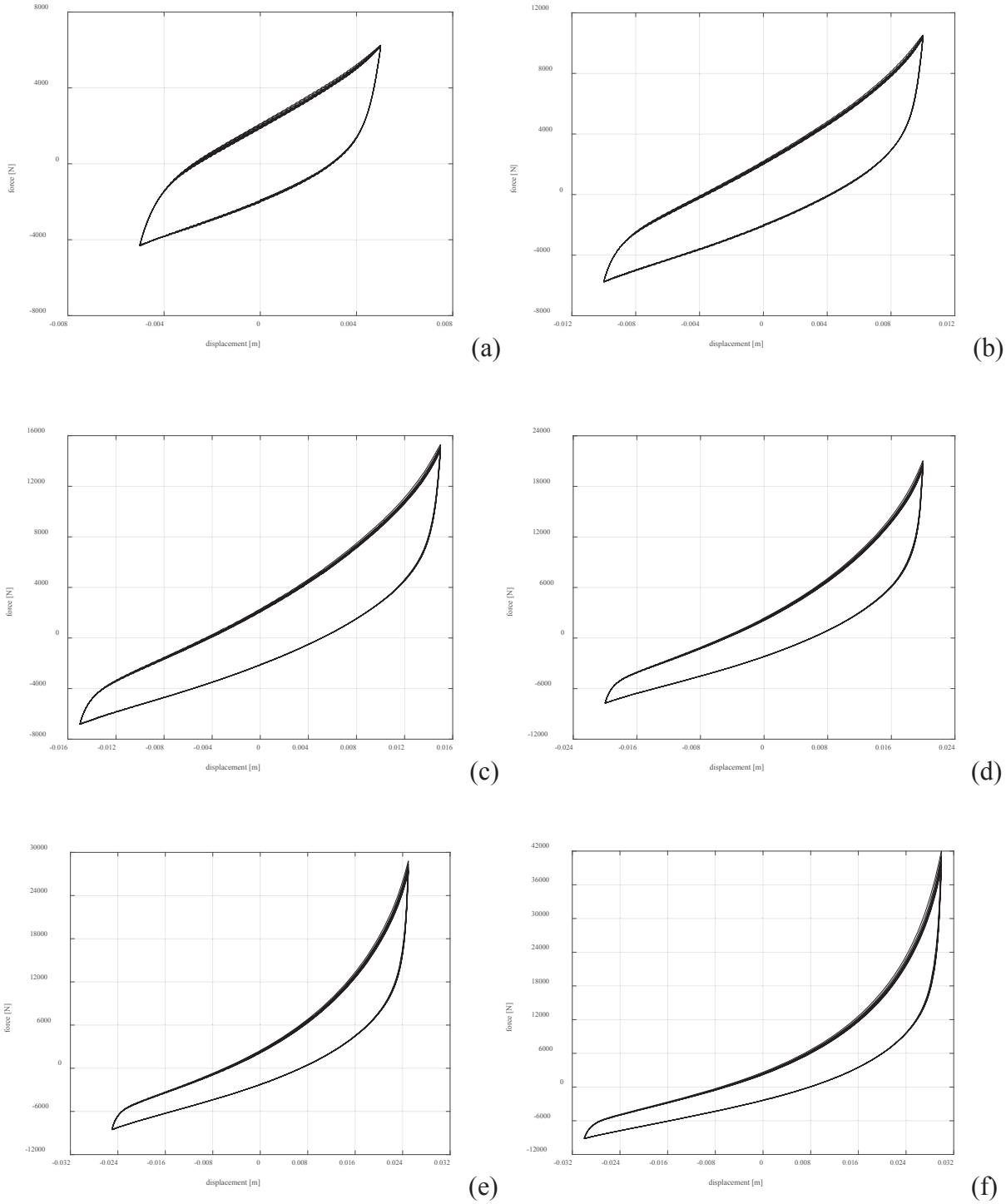

Figure 3: Force-displacement hysteresis loops of HWRI PWHS 16040 at different displacement amplitudes in C/T direction, for Pv = 0 kN and f = 0.1 Hz: (a) ±5, (b) ±10, (c) ±15, (d) ±20, (e) ±25, (f) ±30.

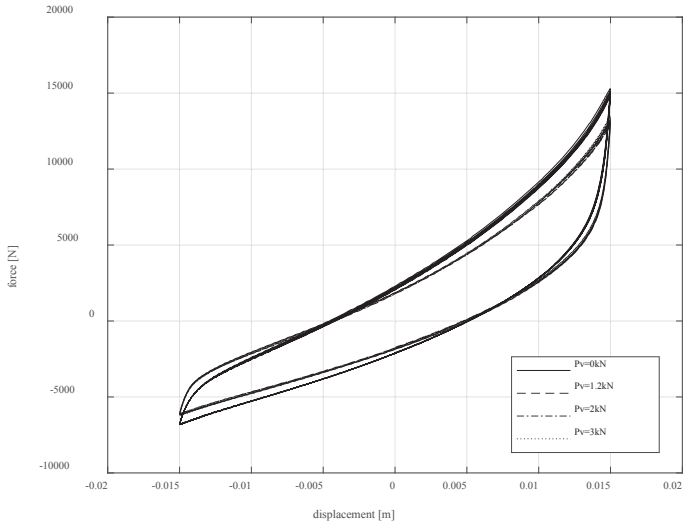

Figure 4: HWRI PWHS 16040: Influence of vertical pre-load at A = 15 mm in Compression/Tension direction.

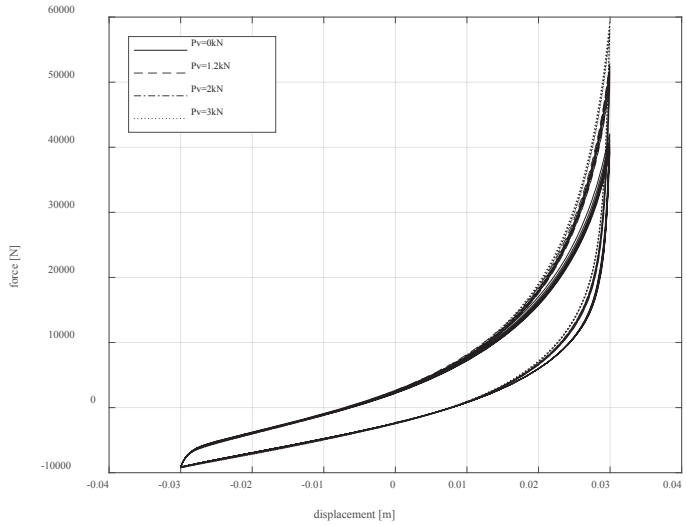

Figure 5: HWRI PWHS 16040: Influence of vertical pre-load at A = 30 mm in Compression/Tension direction.

Figures 4 and 5 show the asymmetric force-displacement hysteresis loops obtained in Compression/Tension direction, under the effect of different values of vertical pre-load, at the displacement amplitudes A = 15 mm (Figure 4) and A = 30 mm (Figure 5). It can be observed that at the largest displacements, the applied vertical pre-load affects much less the dynamic response of the metal device only on Compression side.

6 NUMERICAL SIMULATION OF THE EXPERIMENTAL BEHAVIOUR

As far as the modeling of the dynamic behavior of HWRIs in the vertical direction is concerned, a Modified Bouc-Wen Model (MBWM) is proposed to predict their response. This analytical model is obtained by modifying the expression of the generalized force (Eq. (4)) of the Bouc-Wen Model (depending on five parameters k_2, k_d, β, γ e n):

$$f_u = k_2 u + z(u) \tag{4}$$

where u is the generalized relative displacement, and $z(u)$ is the hysteretic variable given by solving the following first order differential equation:

$$\dot{z} = \left\{ k_d - \left[\gamma + \beta \cdot \mathrm{sgn}\left(z \cdot \dot{u} \right) \right] |z|^n \right\} \dot{u} \tag{5}$$

The proposed modification of the generalized force:

$$f = -\left(\lambda_1 + \lambda_2 \right) u + e^{(\lambda_1 u)} - e^{(-\lambda_2 u)} + e^{(\eta u)} \left(k_2 u + z \right) \tag{6}$$

allows to simulate the asymmetric behaviour in Compression/Tension direction. The proposed model depends by eight parameters k_2, k_d, n, β, γ, λ_1, λ_2 and η, where the latters λ_1, λ_2 and η are those determining the asymmetry of the loops.

The experimental hysteresis loops, obtained by the dynamic tests performed on the different HWRIs, are compared to those derived by the application of the proposed numerical model: the values of the above eight parameters are calibrated in order to simulate the experimental response for a certain vertical pre-load and all the different displacement amplitudes. In particular, such values are: $k_2 = 1100000$, $k_d = 8500000$, $n = 1$, $\beta = 3000$, $\gamma = 0$, $\lambda_1 = 775$, $\lambda_2 = 630$ and $\eta = 55$.

Figure 6 shows the analytical versus experimental comparison for the HWRI PWHS 16010, subjected to a pre-load of 2 kN, with varying the displacement amplitude as described in Table 2. It demonstrates that the proposed mathematical model can satisfactorily predict the dynamic response in a wide displacement range. This satisfying agreement is achieved by all the tested devices, under the different vertical pre-loads.

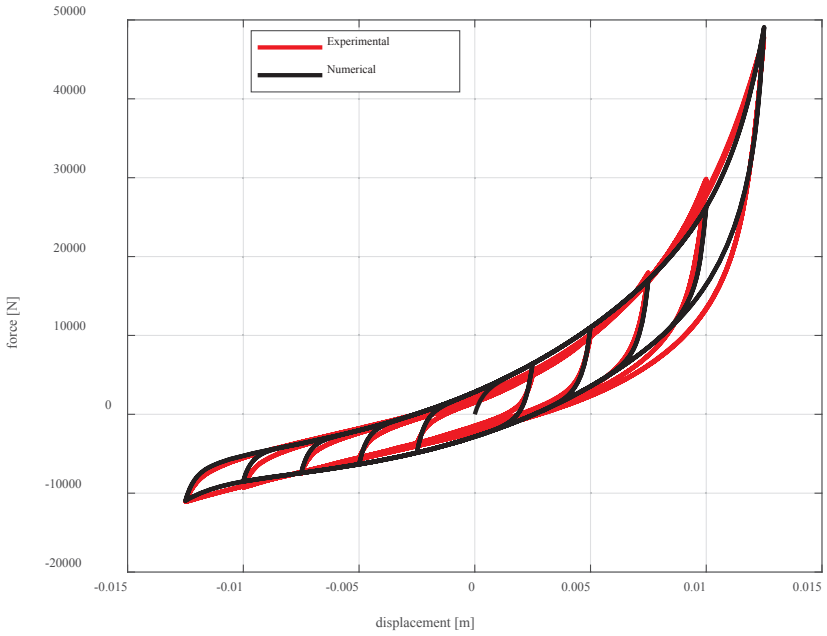

Figure 6: HWRI PWHS 16010: experimental versus numerical hysteresis loops, under a pre-load of 2 kN.

7 CONCLUSIONS

The experimental investigation of the dynamic response of HWRIs, manufactured by Powerflex S.r.l (Limatola, Italy), has been carried out by adopting a testing machine available at the Department of Structures for Engineering and Architecture of the University of Naples Federico II, which allows to impose vertical displacement or load histories to the tested device with a constant vertical pre-load.

Each test consisted in imposing ten cycles of sinusoidal displacement having specified amplitude and frequency, under four different values of vertical pre-load. Six amplitude values have been chosen with the maximum one selected in order to avoid damages to the two alu-

minum alloy retainer bars of the device during the experimental tests. The most investigated loading frequency was assumed equal to 0.1 Hz.

According to the experimental tests results, the tested device is characterized by high effective stiffnesses and equivalent damping ratio in the case of very small imposed displacement amplitudes. These parameters decrease with increasing displacement amplitude, except for the effective stiffness in Tension that dramatically increase towards the largest amplitudes. The shape of the hysteresis loops changes according to the displacements amplitude: at the smallest imposed displacements, the hysteresis loops display a softening stiffness in Compression and a slight hardening in Tension, whereas, at the largest imposed displacements, the device exhibits a hardening stiffness in Tension.

Regarding the effect of the vertical pre-load on the dynamic behavior of the tested HWRI, the experimental outcomes reveal a reduction in the effective stiffness in Compression and an approximately constant equivalent viscous damping ratio due to the increase of the vertical load, while the effective stiffness in Tension increases for the largest amplitudes.

In order to simulate the dynamic behavior of the HWRIs in Compression-Tension direction, a nonlinear model has been proposed, accurately calibrated, and validated by comparing the experimental hysteresis loops provided by cyclic tests with those predicted mathematically. In future papers, it will be necessary to identify a more suitable hysteretic model among those already available in the literature [13-20].

REFERENCES

[1] M.L. Tinker, M.A. Cutchins, Damping phenomena in a wire rope vibration isolation system. *Journal of Sound and Vibration*, **157** (1), 7-18, 1992.

[2] G.F. Demetriades, M.C. Constantinou, A.M. Reinhorn, Study of wire rope systems for seismic protection of equipment in buildings. *Engineering Structures*, **15** (5), 321-334, 1993.

[3] G. Serino, F. Bettinali, G. Bonacina, Seismic base isolation of gas insulated electrical substations: comparison among different solutions. *Proceedings of the 4th US Conference on Lifeline Earthquake Engineering*, San Francisco, California, 1995.

[4] G. Serino, G. Bonacina, F. Bettinali, Passive protection devices for high-voltage equipment: design procedures and performance evaluation. *Proceedings of the 4th US Conference on Lifeline Earthquake Engineering*, San Francisco, California, 1995.

[5] M. Di Donn, G. Serino, Base isolation of high-voltage equipment: comparison between two different solutions. *Proceedings of the 7th International Conference on Probabilistic Methods Applied to Power Systems*, Napoli, Italy, 2002.

[6] S. Alessandri, R. Giannini, F. Paolacci, M. Malena, Seismic retrofitting of an HV circuit breaker using base isolation with wire ropes. Part 1: Preliminary tests and analyses. *Engineering Structures*, **98**, 251-262, 2015.

[7] G. De Canio, Marble devices for the base isolation of the two bronzes of Riace: a proposal for the David of Michelangelo. *Proceedings of the 15th Word Conference on Earthquake Engineering*, Lisbon, Portugal, 2012.

[8] S. Alessandri, R. Giannini, F. Paolacci, M. Amoretti, A. Freddo, Seismic retrofitting of an HV circuit breaker using base isolation with wire ropes. Part 2: Shaking-table test validation. *Engineering Structures*, **98**, 263-274, 2015.

[9] S. Pagano, M. Russo, S. Strano, M. Terzo, A mixed approach for the control of a testing equipment employed for earthquake isolation systems. *Journal of Mechanical Engineering Science*, **228** (2), 246-261, 2014.

[10] A.K. Chopra, *Dynamics of Structures: Theory and Applications to Earthquake Engineering, 4th Edition*. Englewood Cliffs, NJ: Prentice Hall, 2012.

[11] P. Chakrabortty, A.R. Roshan, A. Das, Evaluation of dynamic properties of partially saturated sands using cyclic triaxial tests. *Indian Geotechnical Journal*, Pune, Maharashtra, India, 2015.

[12] S.S. Kumar, A.M. Krishna, A. Dey, Cyclic response of sand using stress controlled cyclic triaxial tests. *Proceedings of the 50th Indian Geotechnical Conference*, **50**, 948-962, 2020.

[13] N. Vaiana, D. Losanno, N. Ravichandran, A novel family of multiple springs models suitable for biaxial rate-independent hysteretic behavior. *Computers & Structures*, **244**, 106403, 2021.

[14] N. Vaiana, R. Capuano, S. Sessa, F. Marmo, L. Rosati, Nonlinear dynamic analysis of seismically base-isolated structures by a novel OpenSees hysteretic material model. *Applied Sciences*, **11** (3), 900, 2021.

[15] N. Vaiana, S. Sessa, L. Rosati, A generalized class of uniaxial rate-independent models for simulating asymmetric mechanical hysteresis phenomena. *Mechanical Systems and Signal Processing*, **146**, 106984, 2021.

[16] N. Vaiana, S. Sessa, F. Marmo, L. Rosati, A class of uniaxial phenomenological models for simulating hysteretic phenomena in rate-independent mechanical systems and materials. *Nonlinear Dynamics*, **93** (3), 1647-1669, 2018.

[17] D. Pellecchia, S. Sessa, N. Vaiana, L. Rosati, Comparative assessment on the rocking response of seismically base-isolated rigid blocks. *Procedia Structural Integrity*, **29**, 95-102, 2020.

[18] N. Vaiana, S. Sessa, M. Paradiso, F. Marmo, L. Rosati, An efficient computational strategy for nonlinear time history analysis of seismically base-isolated structures. *Proceedings of XXIV AIMETA Conference 2019. Lecture Notes in Mechanical Engineering*, 2020. https://doi.org/10.1007/978-3-030-41057-5_108

[19] N. Vaiana, S. Sessa, M. Paradiso, L. Rosati, Accurate and efficient modeling of the hysteretic behavior of sliding bearings. *Proceedings of the 7th ECCOMAS Thematic Conference on Computational Methods in Structural Dynamics and Earthquake Engineering (COMPDYN 2019)*, 2019. https://doi.org/10.7712/120119.7304.19506

[20] S. Sessa, N. Vaiana, M. Paradiso, L. Rosati, An inverse identification strategy for the mechanical parameters of a phenomenological hysteretic constitutive model. *Mechanical Systems and Signal Processing*, **139**, 106622, 2020.